JACS
JOURNAL OF THE AMERICAN CHEMICAL SOCIETY
Article
pubs.acs.org/JACS

Model for Photoinduced Bending of Slender Molecular Crystals

Naba K. Nath,[†] Ljupčo Pejov,[‡] Shane M. Nichols,[§] Chunhua Hu,[§] Na'il Saleh,[⊥] Bart Kahr,[§] and Panče Naumov*[,†]

[†]New York University Abu Dhabi, P.O. Box 129188, Abu Dhabi, United Arab Emirates

[‡]Institute of Chemistry, Faculty of Natural Sciences and Mathematics, Ss. Cyril and Methodius University, MK−1000 Skopje, Macedonia

[§]Molecular Design Institute and Department of Chemistry, New York University, New York, New York 10003−6688, United States

[⊥]Department of Chemistry, College of Science, United Arab Emirates University, P.O. Box 15551, Al Ain, United Arab Emirates

Supporting Information

ABSTRACT: The growing realization that photoinduced bending of slender photoreactive single crystals is surprisingly common has inspired researchers to control crystal motility for actuation. However, new mechanically responsive crystals are reported at a greater rate than their quantitative photophysical characterization; a quantitative identification of measurable parameters and molecular-scale factors that determine the mechanical response has yet to be established. Herein, a simple mathematical description of the quasi-static and time-dependent photoinduced bending of macroscopic single crystals is provided. This kinetic model goes beyond the approximate treatment of a bending crystal as a simple composite bilayer. It includes alternative pathways for excited-state decay and provides a more accurate description of the bending by accounting for the spatial gradient in the product/reactant ratio. A new crystal form (space group $P2_1/n$) of the photoresponsive azo-dye Disperse Red 1 (**DR1**) is analyzed within the constraints of the aforementioned model. The crystal bending kinetics depends on intrinsic factors (crystal size) and external factors (excitation time, direction, and intensity).

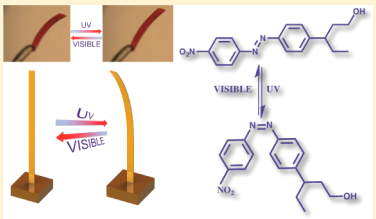

1. INTRODUCTION

Fast energy transfer typical for the dense packing of molecular crystals (relative to soft matter) and the exceptional elasticity of certain slender crystals may lead to the design of rapid, efficient actuators and biomimetic materials.[1−8] The ever-increasing number of reports on crystals that can bend,[5−9] curl,[10−12] twist[13−15] or hop[16−20] when excited with light, suggests that the photomechanical response of molecular single crystals is a more common phenomenon than has been recognized in the past. Indeed, it has been demonstrated recently that slender crystals of practically all major photochromic classes are capable of elastic and reversible mechanical deformation under photoexcitation.[21−31]

The growing number of such examples necessitates the identification of measurable parameters for the quantification and comparison of similar mechanical phenomena from one material to the next. Detailed theoretical models have been already developed for deformation of dye-doped photoactive polymers (mainly elastomers and liquid crystals),[32−37] and qualitative considerations of the effects of crystal shape and size on the mechanical response have been advanced for individual crystalline systems,[38] but general models are not available for describing the actuating capability of single crystals. In the absence of common analytical methods to study kinematic effects, conclusions are based on limited data and are not generally applicable. Under such circumstances, one normally resorts to analogies with the kinematic models that are available for polymeric actuators. Although they are exceedingly convenient, such implicit or explicit analogies are not always justified due to the denser and more uniform distribution of photoactive species, higher degree of coupling of the structure and mechanical energy, and faster time scales for energy transfer in single crystals relative to polymers.

The photoinduced bending of single crystals is regularly attributed to nonuniform conversion, that is, the evolution of a spatial gradient of the product population in the crystal following photoexcitation. The structural misfit of the product and the reactant creates a residual strain that causes macroscopic flexure of the crystal. It is essential to establish measurable parameters that will quantify the factors that affect the resultant internal strain, the extent of crystal deformation, and the kinetics of the macroscopic reshaping.

As part of our efforts to advance the understanding of bending crystals, herein we report the results of an in-depth kinematic analysis of the bending of a molecular crystal, the azo-dye Disperse Red 1 (**DR1**, Chart 1).[39] We observed recently that crystals of **DR1** appear from ethanol solution as planks that frequently bend by as much as 90° when they encounter an obstacle. Under continuous ultraviolet (UV) excitation, the crystals undergo additional instantaneous bending, most likely as a result of the photoinduced *trans*−*cis* isomerization at the azo functionality which is a common characteristic of azo dyes of this kind.[21,22] Crystals bent during

Received: October 3, 2013
Published: January 23, 2014

   dx.doi.org/10.1021/ja4101497 | J. Am. Chem. Soc. 2014, 136, 2757−2766

Chart 1. Chemical Structure of the Azo-Dye Disperse Red 1 (DR1)

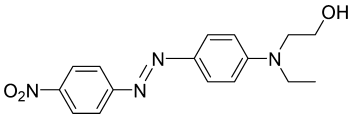

growth with a range of curvatures provide a basis for studying the effects of plastic deformations on the photoelastic response. By kinematic analysis of a series of crystals and under different excitation conditions, we attempted to disentangle the dependence of the bending on both intrinsic, morphological factors (the size and initial shape of the crystal) and external factors (excitation power, direction, and time).

2. RESULTS AND DISCUSSION

2.1. Crystal and Molecular Structure of a New Polymorph of DR1. **DR1** was purchased from Sigma Aldrich and recrystallized once from ethanol by slow evaporation (Figure 1). The crystal planks were elongated along ⟨010⟩. The

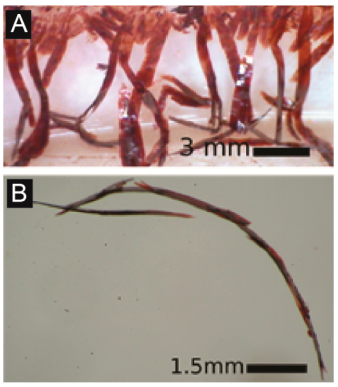

Figure 1. Crystals of form II **DR1**. (A) Crystals bending as they collide with the bottom of the crystallization dish. (B) Single bent conglomerate of crystals unobstructed.

plank faces were {001} and the width was ⟨100⟩. Anhydrous crystals were analyzed by X-ray diffraction at 100 K. **DR1** crystallizes in the space group $P2_1/n$ with a = 10.152(2), b = 7.769(2), c = 38.639(8) Å, β = 92.863(3)°, and Z = 8 (Figure 2). There are two molecules in the asymmetric unit, one of which shows statistical disorder of the ethyl and hydroxyethyl groups.

Figure 2 shows the packing of **DR1** molecules in the unit cell. Along the c direction there are no O···O distances consistent with hydrogen bonding. Some distances appear too small as artifacts of the disorder, while others are too large. On the other hand, there are O···O contacts in other directions consistent with strong H-bonds that underlie the elongation of the crystal

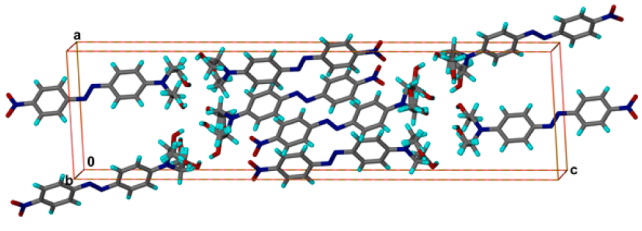

Figure 2. Unit cell packing of form II **DR1**.

morphology along b and the tendency to bend around a during the crystal growth (for details of the crystal structure, see the Supporting Information).

2.2. Bending Crystals of DR1. Ten crystals of **DR1** with curvatures that ranged from practically straight to significantly bent were hand-selected under an optical microscope for kinematic analysis (Figure S1 in the Supporting Information). The crystal size was measured from prerecorded still photographs. The crystal width (a_{cr}) and thickness (b_{cr}) were averaged over three measurements, and the length of the crystals along the curved axis (l) was calculated from their depth (h_{cr}) and chord length (r, identical with the radius of deflection; see below). The radius (R) of the crystal and its curvature ($\kappa = 1/R$) were calculated[40] as $R = (r^2 + 4h_{cr}^2)/8h_{cr}$ and $\kappa = 8h_{cr}/(r^2 + 4h_{cr}^2)$ (Figure 3A). The values of the basic metrics are summarized in Table S1 in the Supporting Information).

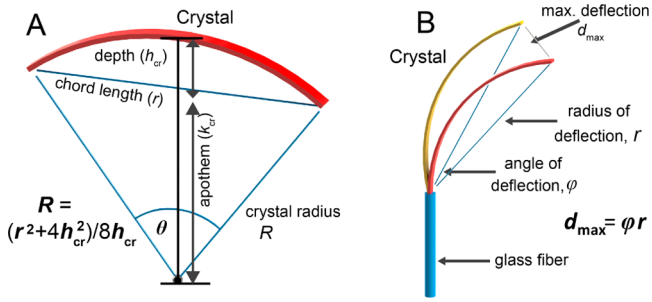

Figure 3. Schematic representation of photoinduced bending of a slender crystal and definition of metric parameters. The relation $d_{max} = \varphi r$ is a reasonable approximation for small bending angles such as those that we observed with **DR1**.

2.3. Quantitative Kinematic Analysis of the Photoinduced Flexure of DR1 Crystals. With the use of a minimum amount of glue, each of the 10 crystals was affixed by one terminus to a glass rod with the vertical direction as {001}/{00$\bar{1}$} in nearly identical positions (Figure S6, Supporting Information). The crystals were exposed in succession to unfocused, continuous wavelength (cw) UV light from a medium-pressure Hg lamp (Figure S1, Supporting Information).[41] With the use of a digital camera coupled to a transmission-mode optical microscope, a series of movies with frame resolution 30 s^{-1} were recorded by exposing the flat face {001}/{00$\bar{1}$} of the crystal to unfiltered UV light during ∼1 s (the exact exposure time was retrieved from the recordings) and individually analyzed. The mechanical response was recorded by exciting each of the concave (cc) and convex (cx) faces of the crystal and by varying the power of the incident light between 0% and 100% of the maximum power in increments of 10% (the exact excitation power at the crystal position was obtained by independent measurement and calibration). The kinematic analysis was performed by tracing the movement of the tip of the crystal from the 2D recordings. Because the crystals did not twist significantly around their longest axis during the deformation, this value also represents bending of the crystal in space. The *relative* deflection related to the movement of the tip of the crystal (d_{rel}) for angle φ around the anchoring point to the base was calculated as $d_{rel} = [(x_2 - x_1)^2 + (y_2 - y_1)^2]^{1/2}$, where $x_{1,2}$ and $y_{1,2}$ are the x and y coordinates of any two consecutive points on the 2D trajectory of the crystal tip extracted from the recordings.

dx.doi.org/10.1021/ja4101497 | J. Am. Chem. Soc. 2014, 136, 2757−2766

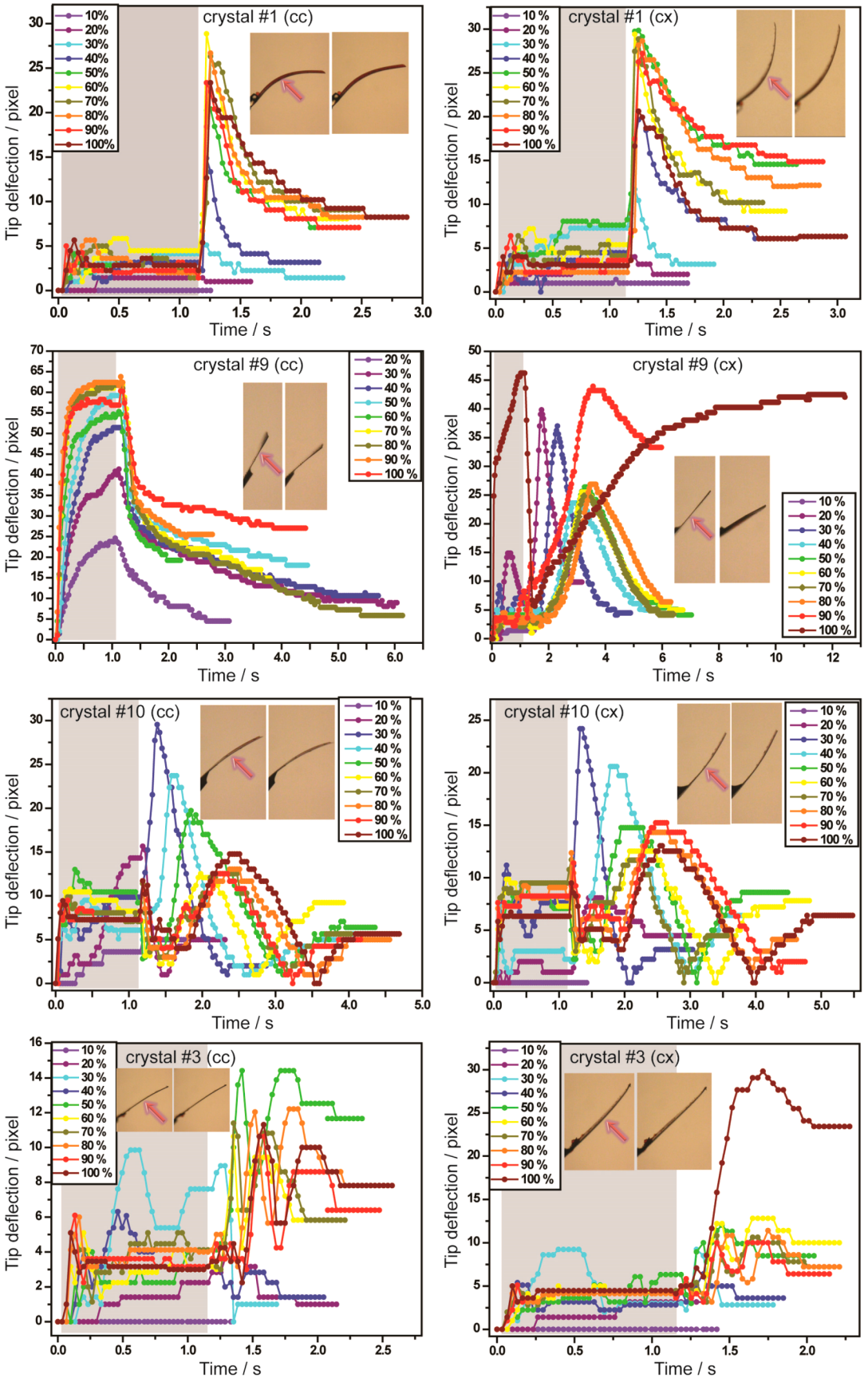

Figure 4. Overlapped time profile of the tracked tip motion of four **DR1** crystals excited with UV light of continuous wavelength (the values in the insets refer to the relative power of the UV light). The arrows show the direction of excitation. The acronyms cc and cx refer to excitation of the concave and convex side of the crystal, respectively.

dx.doi.org/10.1021/ja4101497 | J. Am. Chem. Soc. 2014, 136, 2757−2766

Upon excitation, the crystals rapidly bent in response to the *trans*–*cis* isomerization with estimated conversion yield of <10% . Figure 4 contains representative plots of the trajectories of four crystals excited on both sides at varying incident power (the individual trajectories are shown in Figure S2 and Figure S3 in the Supporting Information). Regardless of whether the crystals were irradiated on their concave (cc) or convex (cx) side, some crystals deflected strongly *during* the exposure to UV light. Except for very high excitation power in some specimens, the bending was reversible; once the irradiation was terminated, the crystals quickly straightened back to their original shape as the *cis* form isomerized back to the *trans* form. In most cases the shape recovery was complete within 5 seconds. Crystal #9 irradiated on its concave (cc) side in Figure S2 shows this type of bending (bending mode **B** hereafter).[42] Other crystals bent only slightly during excitation, but deflected much more *after* the irradiation was terminated, sometimes oscillating several times before they returned to their original shape (bending mode **A**). In either case, except at very high excitation powers, the bending was reversible, although the recovery of the original shape was achieved either gradually or through several ($\leq$3) dampened oscillations. Out of 10 crystals that were examined, seven bent in the same way when irradiated on the cc and the cx sides. Of these seven, four bent in mode A (**A**–**A**) and three in mode B (**B**–**B**). Three crystals exhibited different response (**A**–**B** or **B**–**A**) when excited on opposite sides of the crystal (Table S2, Supporting Information). The etiology of this complex and varied behavior resides in part in the lamellar architectures of multilayered ensembles of planks (Figure 1).

2.4. Dependence of the Bending on the Excitation Power. Figure 5 shows the dependence of crystal bending on the power of the incident light for crystals #1 (**A**–**A**), #3 (**A**–**A**), #9 (**B**–**A**), and #10 (**A**–**A**). The higher excitation power does not always correspond to stronger deflection. For low excitation energies, in response to the increased photoyield of the *cis* form at the incident surface, the crystal bending increases almost linearly with the power density until it reaches a crystal-specific maximum or a plateau from 15–25 mW cm^{-2}. For weak excitations (slight bending), the deflection of the crystal is nearly proportional to the light intensity. The strongest deflection is related to the highest possible conversion at the surface layer of the irradiated crystal face, as determined by the absorption characteristics of the crystal. Excitation at higher power does not increase the flexion; in fact, in most cases, the crystal bends less, likely as a result of the filtering effect from the photoinduced *cis* form and/or decomposition of the photoproduct. Occasionally, at very strong excitation power, we observed plastic deformation of the crystal. Nevertheless, the crystal integrity was preserved in all cases and we did not observe any apparent deterioration.

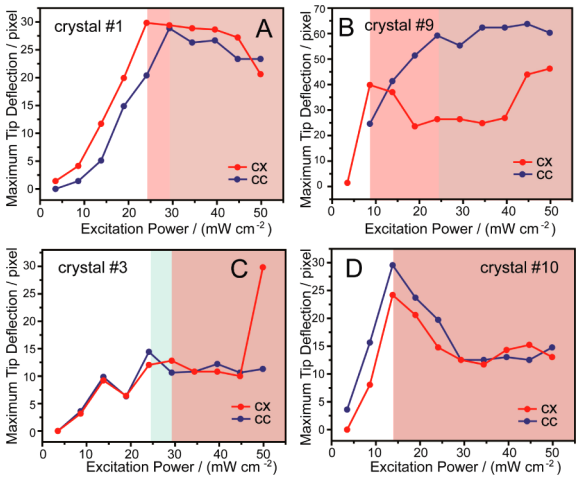

Figure 5. Dependence of the bending on the excitation power for four **DR1** crystals irradiated on their concave (cc) and convex (cx) sides. The shaded regions represent regimes where the increased power alleviates the crystal deflection.

The excitation profile of the bending for each crystal also reflected the mode of bending. As shown in Figure 5A,C,D, in case of crystals that exhibit the same bending mode when excited on both faces (#1, #3 and #10, all in **A**–**A** mode) the power dependence was the same on both faces. On the contrary, when excited on two faces, crystal #9 (**B**–**A** mode, Figure 5B) showed different power dependencies.

2.5. Dependence of the Bending on the Crystal Size. To obtain insight into the bending variability, we correlated the degree of deflection with the crystal length (l), thickness (b_{cr}) and width (a_{cr}) for crystals that bent in modes A and B when irradiated on their cc and cx faces. Since the maximum absolute deflection distance d_{max} is determined foremost by the crystal length, we used the deflection angle of the crystal tip φ as a comparative measure of deformation. To simplify the analysis, for the small deflections observed with **DR1**, as a first approximation we can assume that the curvature of the crystal ($\kappa = 1/R$) and thus the radius of deflection (r) are constant.

We consider the maximum deflection angle φ for a certain crystal over *all values* of the excitation power (Figure 6) and the deflection at identical excitation power (in Figure 7, the power is 292.4 mW cm^{-2}). Since in the former case φ refers to the maximum deflection extracted from bending at different excitation powers, these correlations reflect the physical limits for photoinduced bending of crystals of **DR1**. In the case of identical power, the deflection provides direct comparison among different crystals. Comparison of the size effect on the deflection at *identical power* for all crystals eliminates the contribution from the power density of incident excitation and provides a more realistic measure of the effects of crystal size. Not surprisingly, the two plots are very similar.

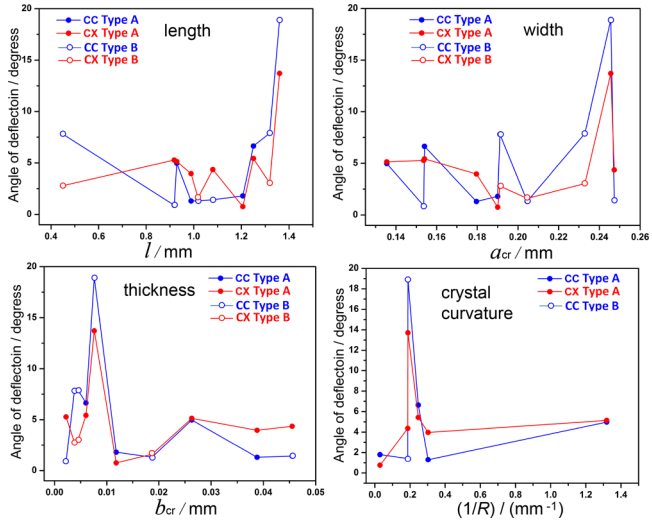

Figure 6. Effect of crystal size and curvature on the maximal deflection angle of **DR1** crystals.

dx.doi.org/10.1021/ja4101497 | *J. Am. Chem. Soc.* 2014, 136, 2757–2766

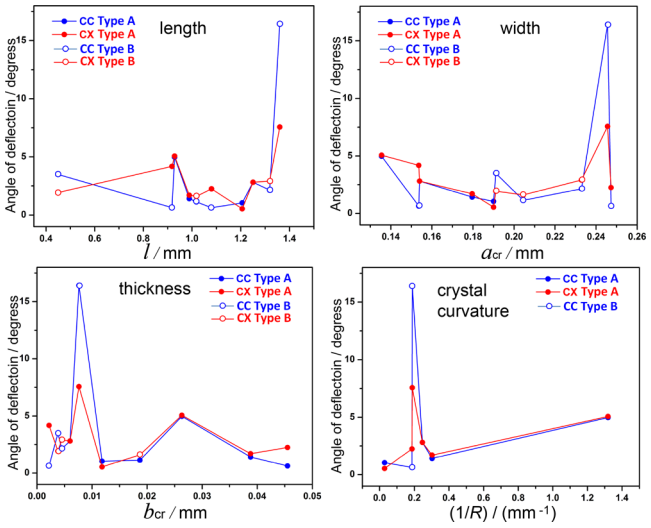

Figure 7. Effect of crystal size and curvature on the deflection angle of **DR1** crystals at fixed incident power of 292.4 mW cm^{-2}.

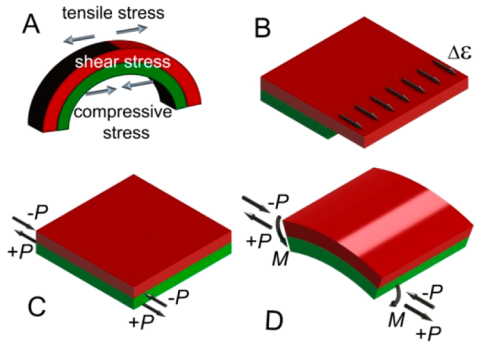

Figure 8. Forces and stresses involved in bending of a crystal bilayer as model for photoinduced crystal bending, under application of a lateral load. The load results in evolution of tensile and compressive stresses on the opposite sides of the bilayer, and shear stresses along the direction of the load (A) that are equivalent to an ideally uniform misfit strain, $\Delta\varepsilon$ (B). This strain can be compensated by applying to the two layers forces P in opposite directions (C) that ultimately creates a bending moment M (D) and appears as macroscopic bending of the bilayer.

From Figures 6 and 7 it appears that the maximum deflection is achieved with very long (large l) and wide (large a_{cr}), but thin (small b_{cr}) crystals. Longer crystals (large l) bend better because the crystal mass at larger distance contributes with a larger moment of inertia. Thicker crystals (large b_{cr}), on the other hand, are usually stiffer; the bending moment[43] is thus transferred less efficiently along the crystal. Correlation with the crystal thickness (b_{cr}), however, indicates a more complex trend; the deflection increases with thickness, the strongest bending occurs around $b_{cr} \sim 0.008$ mm, and decreases for wider crystals. This observation could be a result of two counterbalanced influences, the width of the plank and the stiffness. Because the crystals in these experiments are irradiated on their flat side, narrower crystals are expected to bend less because of smaller area available for absorption of photons where the bending momentum is created. Likewise, the photon absorption is more effective in wider crystals, but wider crystals are usually thicker and stiffer. A similar trend is observed for the crystal curvature, κ (Figures 6 and 7), where the maximum deflection occurs around $\kappa \sim 0.22$ mm^{-1}. This result contradicts the intuitive expectation that crystals which were originally bent (large κ) would bend less by photoexcitation. We could not determine any clear difference between crystals that bend according to mode A and mode B.

2.6. Theoretical Models for the Photoinduced Bending. Loads that are applied laterally to the longitudinal axis of slender crystals induce two types of stress that appear on the bending and expanding faces of the crystal: *shear* stress that evolves along the direction of the applied force, and *compressive* and *tensile stresses* that develop orthogonal to it (Figure 8A).[44] The exact description of the resulting *quasistatic* (time-independent) deformations is provided by the Euler-Bernoulli theory for bending of slender beams.[45] This general description is improved by accounting for the effects of shearing within Timoshenko's approach.[46−49]

Time-resolved fluorescence spectroscopic measurements showed that the lifetimes of the photoinduced *cis* forms of the two molecules in **DR1** in the crystal are 0.07 ns (a_i = 94%) and 2.19 ns (a_i = 6%) (the emission spectrum of the crystal, the fluorescence decay curves and the related parameters are available as Figure S4 and Table S3 in the Supporting Information). Thus, the bending of the crystals, which occurs on time-scale of <0.1 s is related to response of the material to decay of the de-excited *cis* form to the *trans* form. This reaction induces the bending as a latent, macroscopic mechanical effect. According to the currently widely accepted, qualitative mechanism, the photoinduced bending of molecular crystals occurs as a mechanical response to internal stress emanating from the product/reactant gradient along the crystal depth. In the ideal case of entirely homogeneous solid-state processes (that is, in the absence of phase separation) and in line with the Beer−Lambert law, the product/reactant ratio changes gradually as a result of absorption of light by the material. As a result, ultimately a mixed crystal of the reactant with spatially nonuniform and gradually decreasing molar ratio of the product is obtained. The attempts to determine the conversion yield in photomechanically responsive crystals have established that high *overall* photoconversion is not a prerequisite for a mechanical response by photoactive crystals. Indeed, mechanical responses were reported with molar yields as small as 2−5%;[22] instead, sufficient *local* conversion at the exposed crystal surface is required for a spatial concentration gradient of product molecules. Estimated values for the conversion of 50−100% within the reactive surface layer are not uncommon.[50]

The bending of a very thin model crystal of length l that was initially straight and parallel to the x axis is measured and quantified by the *deflection angle*, φ (Figure 9). Because the

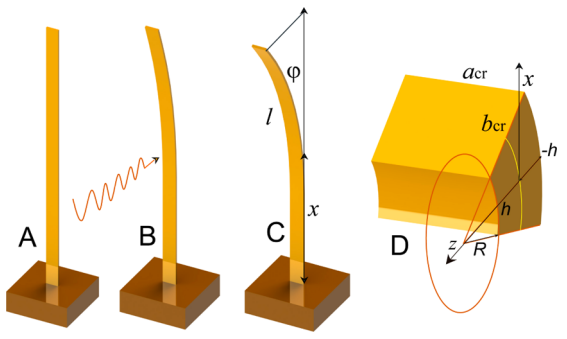

Figure 9. A model for photoinduced bending of slender crystal and definition of the related parameters.

dx.doi.org/10.1021/ja4101497 | J. Am. Chem. Soc. 2014, 136, 2757−2766

angle (expressed in radians) is given by the ratio between the respective arc length and the radius of the circle that approximates the crystal curvature, the total deflection angle is given by an integral, over the crystal length, of the ratio between the distance and the deflection angle, $[1/R(x)]\cdot dx$,[5] starting from the anchor point:

$$\varphi = \int_0^l \frac{dx}{R(x)} \tag{1}$$

In the very simplified albeit intuitive model described above (Figure 8), a partially transformed crystal effectively acts as a bimetallic strip, where a misfit in the thermal expansion of the two phases induces residual strain around the phase boundary.[51,52] The application of stress by conversion of the reactive layer to the product causes its expansion and induces uniaxial misfit strain ($\Delta\varepsilon$). This misfit strain can be compensated for by applying a pair of opposing forces ($-P$ and P) thereby inducing a residual bending moment M.[43] The curvature of the bent crystal, κ, defined as reciprocal radius ($1/R$) of a circle moving tangentially across its surface, is given by the ratio of the bending moment M and the crystal stiffness, Σ:

$$\kappa = \frac{1}{R} = \frac{M}{\Sigma} \tag{2}$$

Depending on whether a sharp or diffuse phase boundary between the reactant and product phases is considered, one of two approaches can be advanced, enabling at least in principle, the calculation of the curvature: (a) discrete quasistatic photoinduced bending, and (b) continuous quasistatic photoinduced bending. The underlying principles of these models are described in the Supporting Information. The first model is clearly inadequate for description of the deformation because it assumes a discontinuous change of the elastic properties at a hypothetical phase boundary between an unreacted phase and a completely reacted phase. The second model of Yakobson and Boldyreva[5] appears to be more appropriate, although in the original form it does not account for the time profile of the deformation. Here, we built up on the second quasistationary model by introducing into the picture the kinetics of the underlying photochemical events.

2.7. Dynamic Photoinduced Bending of Single Crystals. *2.7.1. A Simple Kinetic Model.* We start by setting a description for the crystal deflection (an observable physical quantity) as a function of time in the two light regimes—during illumination (hereafter, "light stage"), and after the illumination has been terminated ("dark stage"). The deflection (bending) angle of the crystal with length l is given by eq 1. However, in this form, eq 1 describes the deformation at a given instant of the time, t. To relate the deflection angle to the kinetics of the photochemical transformation, we generalize eq 1 as a function of time:

$$\varphi(t) = \int_0^l \frac{dx}{R(x,\, t)} \tag{3}$$

Hereafter, we assume that the bending of the crystal has been caused solely as a latent mechanical response to a photochemical transformation (i.e., in absence of external elastic forces that would contribute to the bending). The radius of curvature at a given point x, upon illumination of the sample accompanied by a degree of conversion α, that further induces its deflection from the initial orientation, is given by

$$\frac{1}{R_\alpha} = \frac{M_\alpha}{a_{cr} Y_0 \int_{-h}^{h} z^2\, dz} \tag{4}$$

where

$$M_\alpha = -v a_{cr} Y_0 \int_{-h}^{h} \alpha(z) z\, dz \tag{5}$$

In eq 5, Y_0 is the Young's modulus of the material, a_{cr} is the crystal width, and v is the coefficient of volume expansion. In absence of external forces, the distribution of α is given by the Beer–Lambert's law

$$\alpha(z) = \alpha_0 \exp\left(-\frac{z+h}{d}\right) \tag{6}$$

where d is the characteristic depth of light absorption of the sample (Figure 9D).

Inclusion of the kinetic factor in eq 6 requires assumptions related to the photochemical kinetics. In the simplest possible case of first-order kinetics,

$$S' \xrightarrow{k_1} S'' \tag{7}$$

the solutions of the corresponding kinetic equations lead to the following time-dependence of the concentrations of the reactant and the product:

$$c_{S'}(t) = c_{S',0} \exp(-k_1 t) \tag{8}$$

$$c_{S''}(t) = c_{S',0}[1 - \exp(-k_1 t)] \tag{9}$$

The degree of conversion at each value of z at time t is then

$$\alpha(t) = \frac{c_{S''}(t)}{c_{S',0}} \tag{10}$$

Accounting for eqs 8 and 9, we obtain

$$\alpha(t) = 1 - \exp(-k_1 t) \tag{11}$$

Thus, α depends on t and z according to

$$\alpha(z,\, t) = \alpha_0 \exp\left(-\frac{z+h}{d}\right)[1 - \exp(-k_1 t)] \tag{12}$$

Substituting eq 11 in 4 and then 3, we arrive at

$$\frac{1}{R_\alpha(t)} = \frac{3d^2 v}{2h^3}\left(\frac{h}{d} - 1\right)\left[\exp\left(\frac{2h}{d}\right) - 1\right][1 - \exp(-k_1 t)] \tag{13}$$

It follows from the explicit form described by eq 13 that within the simplest kinetic model of photochemical transformation, the time-dependence of φ during the light stage is governed by

$$\varphi(t) \propto [1 - \exp(-k_1 t)] \tag{14}$$

We introduce reversibility into this model by assuming that after the excitation has been terminated, S″ transforms back to S′:

$$S'' \xrightarrow{k_{-1}} S' \tag{15}$$

Assuming first-order kinetics for the reverse reaction, the time profile of the product will be governed by an exponential decay function:

$$\alpha(t) \propto \exp(-k_{-1} t) \tag{16}$$

$$\varphi(t) \propto \exp(-k_{-1} t) \tag{17}$$

dx.doi.org/10.1021/ja4101497 | J. Am. Chem. Soc. 2014, 136, 2757–2766

Therefore, the implementation of the simplest kinetic model of phototransformation into the theory of photoinduced crystal bending leads to the conclusion that during the light stage the crystal bends with time as $[1 - \exp(-k_1 t)]$. After termination of irradiation, the crystal straightens exponentially and proportionally to $\exp(-k_{-1} t)$.

2.7.2. Extended Kinetic Model. We now consider a more rigorous and also more general model for the kinetics of a photochemical transformation based on the photodecay scheme

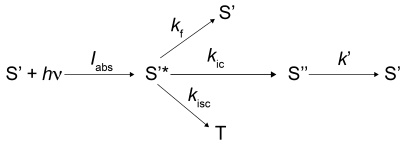

(18)

where the primary absorption by S′ leads to the excited state S′*, whose decay branches through three channels, fluorescence (f), internal conversion (ic) and intersystem crossing (isc), each obeying first-order kinetics. All kinetic equations for this scheme (mostly first-order differential equations) have analytical solutions (for details, see the Supporting Information). In the context of photoinduced crystal bending, we are primarily interested in the internal conversion channel, so we focus here on the time-dependence of $c_{S''}$. By solving the corresponding system of differential equations, the product concentration $c_{S''}$ during the light stage is governed by the following equation:

$$c_{S''}(t) = \frac{k_{ic}}{k} I_{abs}\left[\frac{1 - \exp(-k't)}{k'} - \frac{\exp(-kt) - \exp(-k't)}{k' - k}\right] \tag{19}$$

When $k' \ll k$, all exponential terms in eq 19 may be expanded in a McLaurin series, and the expression reduces to

$$c_{S''}(t) = \frac{k_{ic}}{k} I_{abs}\left[\frac{k'}{k}t + \frac{1}{2!}\left(k - \frac{k'^2}{k}\right)t^2 + \frac{1}{3!}\left(\frac{k'^3}{k} - k^2\right)t^3 + \cdots\right] \tag{20}$$

where k is given by

$$k = k_{ic} + k_{isc} + k_f \tag{21}$$

By solving the corresponding system of differential equations for the dark stage, one arrives at the following expression for $c_{S''}(t)$:

$$c_{S''}(t) = \frac{k_{ic}}{k' - k} c_{S^*,ss} \exp(-kt) + \left(c_{S'',ss} - \frac{k_{ic}}{k' - k} c_{S^*,ss}\right) \exp(-k't) \tag{22}$$

Equation 22 shows that within the framework of this model, the time-dependence of $c_{S''}$ after termination of the light excitation is governed by a double exponential function. Analogous relations hold for $\varphi(t)$. Equation 19 can also be helpful for deducing the dependence of φ on the intensity of excitation light.

In addition to the pathways in eq 18, we have considered a more complex kinetic scheme that includes alternative decay route from the triplet state to S″ (eq 23)

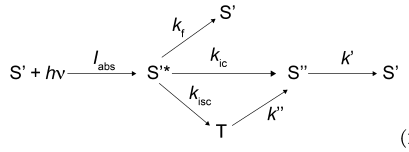

(23)

The kinetic equation

$$\frac{dc_{S''}}{dt} = k_{ic} c_{S^*} + k'' c_T - k' c_{S''} \tag{24}$$

can be solved by using analogous approach (detailed in the Supporting Information) for the light stage:

$$\begin{aligned} c_{S''}(t) = {} & \frac{I_{abs}}{k \cdot k'}(k_{isc} + k_{ic})[1 - \exp(-k't)] \\ & + \frac{k_{isc} I_{abs}}{(k' - k'')(k'' - k)}[\exp(-k''t) - \exp(-k't)] \\ & + \frac{k'' k_{isc} I_{abs}}{k(k' - k)(k'' - k)}[\exp(-k't) - \exp(-kt)] \\ & + \frac{k_{ic} I_{abs}}{k(k' - k)}[\exp(-kt) - \exp(-k't)] \end{aligned} \tag{25}$$

The reverse motion in the dark stage is then described by

$$c_{S''}(t) = A_1 \exp(-k't) + A_2 \exp(-kt) + A_3 \exp(-k''t) \tag{26}$$

where

$$A_1 = c_{S'',ss} - \frac{1}{k' - k}\left(k_{ic} c_{S^*,ss} + \frac{k'' k_{isc} c_{S^*,ss}}{k'' - k}\right) - \frac{1}{k' - k''}\left(k'' c_{T,ss} + \frac{k'' k_{isc} c_{S^*,ss}}{k'' - k}\right) \tag{27}$$

$$A_2 = \frac{1}{k' - k}\left(k_{ic} c_{S^*,ss} + \frac{k'' k_{isc} c_{S^*,ss}}{k'' - k}\right) \tag{28}$$

$$A_3 = \frac{1}{k' - k''}\left(k'' c_{T,ss} + \frac{k'' k_{isc} c_{S^*,ss}}{k'' - k}\right) \tag{29}$$

Thus, although being nontrivial from a mathematical viewpoint (from the aspect of solving the corresponding differential kinetic equations), generalization by explicit inclusion of the T → S″ reaction channel is possible, and the final effect is inclusion of additional exponential-decay term in $c_{S''}(t)$ in the dark stage. The only difference of this result with that in eq 18 is that the time-dependence of $c_{S''}$ is described by triple instead of double exponential function. The time-dependence of the deflection angle is governed by the same function. As shown below, the double-exponential function in eq 22 affords better fit to the experimental data, and thus appears a more appropriate choice.

2.7.3. Verification of the Models. To confirm the validity of the two models, as well as to assess their performance toward the description of the kinetics of crystal bending, we carried out nonlinear least-squares fitting of the deflection angle, φ. We focus here on crystal #9, which is characterized by relatively simple kinematic behavior (Figure 4) and does not undergo damped oscillations; this might be a result of the crystal #9 being monolithic, unlike the typical **DR1** crystals where the thickness varies slightly along the crystal due to the stacking of very thin layers (Figure 1B).[42] The oscillations appear as a

dx.doi.org/10.1021/ja4101497 | J. Am. Chem. Soc. 2014, 136, 2757−2766

result of the restoring elastic force of the crystal and are not photochemically driven; thus, they are not included in the current photochemical considerations.

Within the simpler (linear kinetics) model for the mechanism of photoinduced transformation, the time-dependent data for $\varphi(t)$ during the light stage were modeled with eq 14, whereas the dark stage is modeled with eq 17. The time-dependence of the angular deflection of a crystal sample in the light stage is shown in Figure 10A together with the fit to a

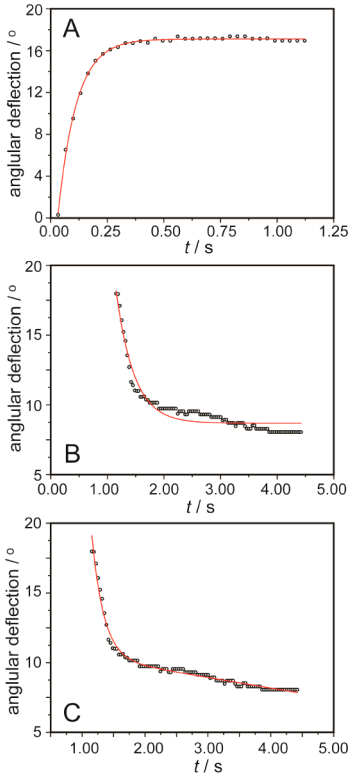

Figure 10. Results of fitting of the deflection angle (φ) of **DR1** crystal (specimen #9)[42] with bending modeled with monoexponential function (A) and of the straightening modeled with monoexponential (B) and biexponential functions (C). The crystal was excited with power density of 500 mW cm^{-2}.

function of the form (14). The bending is clearly a monoexponential process. The motion of the same specimen in the dark stage, together with the fitting function of form (17), is presented in Figure 10B. As can be inferred from there, the experimental time-decay of the angular deflection is not appropriately described by simple linear kinetics. Indeed, the semilogarithmic plot deposited as Figure S5 in the Supporting Information is even more indicative of two distinct time-regimes characterized with different time constants. Therefore, we have fitted the data with a biexponential function (eq 30), implied by the more advanced kinetic model described with eq 22:

$$\varphi(t) \propto A \exp(-kt) + B \exp(-k't) \quad (30)$$

The result from the fit is shown in Figure 10C. The improvement of the agreement between the model and the experimental data is evident from the plot, and is supported by favorable correlation statistics. Indeed, $\varphi(t)$ in the light stage is in excellent agreement with both functions arising from the more advanced model of the form 19 and 20.

2.7.4. Dependence of Bending on the Excitation Power. Within our more general model for bending kinetics of a molecular crystal induced by photochemical transformation described by the reaction scheme 18, we were also able to predict the dependence of the angular deflection on the excitation power. Equations 19 and 20 show that in the case where the conditions for continual transformation of S′ to S″ are fulfilled, $c_{S''}(t)$ is proportional to I_{abs}. Therefore, at any instant when these conditions are fulfilled, φ is also expected to depend linearly on the power of the incident UV excitation. This is in line with the nearly linear dependence of the crystal bending with the power density at relatively lower excitation powers. This linear trend extends to a plateau, corresponding to saturation after reaching the highest possible conversion in the surface layer of the irradiated crystal face (at high concentration of the primary photoabsorption product S*, stimulated emission S* + $h\nu \rightarrow$ S + 2$h\nu$ may also be favored). On the basis of this discussion, we have fitted the dependence of φ on the power of the incident UV light I by the following empirical function:

$$\varphi(I) \propto A[1 - \exp(-aI)] \quad (31)$$

From eq 31, for small values of the incident power I, $\varphi(I)$ is proportional to the power. At high incident power, $\varphi(I)$ is saturated and maximal bending (of ~18°) is expected. In line with these considerations, the fit of the dependence of φ on I in Figure 11 shows close resemblance with the trend of the experimental data (R = 0.967).

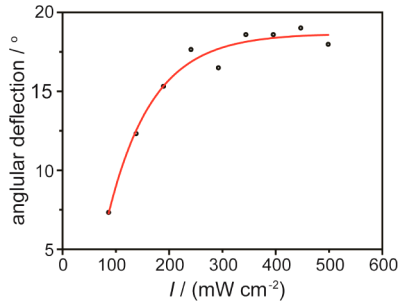

Figure 11. Dependence of the deflection angle (φ) of **DR1** crystal (specimen #9) on the power density of the incident light. The crystal was excited on the concave flat side. The red curve represents the best fit according to eq 31.

2.7.5. Dependence of Bending on the Crystal Thickness. The dependence of the deflection of the crystals on their thickness stands as an important, but rather involved part of the model. From the theoretical side, the models that have been proposed to describe the effect of crystal thickness on the bending regularly employ the crystal curvature (κ) as an indirect measurable (for details, see the Supporting Information). From the basic equations given for the case of discrete phototransformation, a general equation for φ as a function of crystal thickness b_{cr} can be derived (eq 32). The derivation of this relation is straightforward and requires expression of the thicknesses of the reacted and unreacted layers through b_{cr} (i.e., h), and carrying out some tedious algebra (the details are described in the Supporting Information). In eq 32, the constants A, B, ..., H include the Young's moduli of the layers, tensile stresses, and other parameters.

dx.doi.org/10.1021/ja4101497 | J. Am. Chem. Soc. 2014, 136, 2757−2766

$$\varphi \propto \frac{Ab_{cr}^2 - Bb_{cr}}{C + Db_{cr} + Eb_{cr}^2 + Fb_{cr}^3 + Gb_{cr}^4 + Hb_{cr}^5} \quad (32)$$

In the case of continuous phototransformation, with the additional constraint that $d/b_{cr} \ll 1$, where d is a characteristic depth for color evolution, the dependence of φ (and κ) on the crystal thickness is given by

$$\varphi(t) \propto \frac{A}{b_{cr}^2} \quad (33)$$

For thin crystals, the terms of higher order than 3 in b_{cr} can be omitted. Thus, eq 32 reduces to the form:

$$\varphi \propto \frac{Ab_{cr}^2 - Bb_{cr}}{C + Db_{cr} + Eb_{cr}^2 + Fb_{cr}^3} \quad (34)$$

However, nonlinear least-squares fitting of our experimental $\varphi - b_{cr}$ data with model functions of the forms 32−34 were not conclusive, due to the scatter of the experimental data in effect to the natural distribution of the crystal size. Reliable verification of the model requires measurements on a set of crystals where the thickness is systematically varied while the other metrics are fixed. This is a challenging task because it requires strict control over the crystal size aspect ratio which could not be controlled in our crystallization experiments. In addition to the natural distribution of the crystal length and width, small variations in crystal thickness and inhomogeneities expected from the crystal morphology (see above) add to the difficulties with accurate mathematical modeling of this relation in the case of **DR1** crystals.

3. CONCLUSIONS

The growing number of reports on molecular crystals that bend when exposed to light necessitates development of quantitative mathematical models for comparison of their mechanical response in view of their efficacy for conversion of light into mechanical work. The qualitative bilayer model that has been regularly invoked in the past to explain the propensity of crystals to bend does not provide deeper insight into the effects of intrinsic and external factors that direct the mechanical response beyond the mere reason for the occurrence or absence of bending. Here, we describe two versions (simple and extended) of a relatively simple time-dependent mathematical model that explicitly accounts for the gradual profile of the product in the crystal as well as for the time-profiles of the onward and the reversed chemical reaction. Although in its current form the model does not include parameters related to Young's moduli of the crystals, the elastic properties are implicitly accounted for through a set of fitted parameters. Application of the model to a simple case of monotonous deflection and straightening of slender crystals of a new polymorph of the azo-dye **DR1** confirmed its usefulness in describing the kinetics of the bending and unbending, and in modeling the dependence of the deflection angle on the excitation power. When considering future developments, this model would benefit greatly from inclusion of factors that are intrinsic to the crystal and are hardly manageable by experimental control such as the aspect ratio of the crystal metrics.

■ ASSOCIATED CONTENT

Supporting Information

Detailed mathematical procedures, crystal metrics (Table S1), bending modes (Table S2), multiexponential decay analysis of the TR spectra (Table S3), snapshots of the bending crystals (Figure S1), temporal profile of the crystal deflection (Figure S2 and S3), fluorescence lifetime traces (Figure S4), semi-logarithmic plot of the deflection angle versus time (Figure S5), face indexing (Figure S6), exemplary recordings of the bending crystals (Movies S1−S20; all movies are available from the authors), and crystallographic data in CIF format. This material is available free of charge via the Internet at http://pubs.acs.org.

■ AUTHOR INFORMATION

Corresponding Author

pance.naumov@nyu.edu.

Notes

The authors declare no competing financial interest.

■ ACKNOWLEDGMENTS

We thank NYUAD for the financial support and Mr. Mark Pierce for his assistance. B.K. thanks the US National Science Foundation (CHE-0845526, DMR-1105000) for support. We thank Mr. Bailey Curzadd for his help with the graphics.

■ REFERENCES

(1) Kobatake, S.; Takami, S.; Muto, H.; Ishikawa, T.; Irie, M. *Nature* **2007**, *446*, 778.
(2) Terao, F.; Morimoto, M.; Irie, M. *Angew. Chem., Int. Ed.* **2012**, *51*, 901.
(3) Ghosh, S.; Reddy, C. M. *Angew. Chem., Int. Ed.* **2012**, *51*, 10319.
(4) Reddy, C. M.; Krishna, G. R.; Ghosh, S. *CrystEngComm* **2010**, *12*, 2296.
(5) Yakobson, B. I.; Boldyreva, E. V.; Sidelnikov, A. A. *Proc. Sib. Dept. Acad. Sci. USSR* **1989**, *51*, 6.
(6) Boldyreva, E. V.; Sidelnikov, A. A.; Rukosuev, N. I.; Chupakhin, A. P.; Lyakhov, N. Z. Patent SU 1368654, 1985.
(7) Good, J. T.; Burdett, J. J.; Bardeen, C. J. *Small* **2009**, *5*, 2902.
(8) Pierpont, C. G. *Proc. Indian Acad. Sci., Chem. Sci.* **2002**, *114*, 247.
(9) Abakumov, G. A.; Nevodchikov, V. I. *Dokl. Akad. Nauk SSSR* **1982**, *266*, 1407.
(10) Stolow, R. D.; Larsen, J. W. *Chem. Ind.* **1963**, 449.
(11) Uchida, K.; Sukata, S.; Matsuzawa, Y.; Akazawa, M.; de Jong, J. J. D.; Katsonis, N.; Kojima, Y.; Nakamura, S.; Areephong, J.; Meetsma, A.; Feringa, B. L. *Chem. Commun.* **2008**, 326.
(12) Kim, T.; Al-Muhanna, M. K.; Al-Suwaidan, S. D.; Al-Kaysi, R. O.; Bardeen, C. J. *Angew. Chem., Int. Ed.* **2013**, *52*, 6889.
(13) Zhu, L.; Al-Kaysi, R. O.; Bardeen, C. J. *J. Am. Chem. Soc.* **2011**, *133*, 12569.
(14) Kim, T.; Zhu, L.; Mueller, L. J.; Bardeen, C. J. *CrystEngComm* **2012**, *14*, 7792.
(15) Shtukenberg, A. G.; Freudenthal, J.; Kahr, B. *J. Am. Chem. Soc.* **2010**, *132*, 9341.
(16) Trommsdorff, H. *Ann. Chem. Pharm.* **1834**, *11*, 190.
(17) Natarajan, A.; Tsai, C. K.; Khan, S. I.; McCarren, P.; Garcia-Garibay, M. A. *J. Am. Chem. Soc.* **2007**, *129*, 9846.
(18) Naumov, P.; Kowalik, J.; Solntsev, K. M.; Baldridge, A.; Moon, J.-S.; Kranz, C.; Tolbert, L. M. *J. Am. Chem. Soc.* **2010**, *132*, 5845.
(19) Colombier, I.; Spagnoli, S.; Corval, A.; Baldeck, P. L.; Giraud, M.; Leaustic, A.; Yu, P.; Irie, M. *J. Chem. Phys.* **2007**, *126*, 011101.
(20) Naumov, P.; Sahoo, S. C.; Zakharov, B. A.; Boldyreva, E. V. *Angew. Chem., Int. Ed.* **2013**, *52*, 9990.
(21) Koshima, H.; Ojima, N. *Dyes Pigm.* **2012**, *92*, 798.
(22) Koshima, H.; Ojima, N.; Uchimoto, H. *J. Am. Chem. Soc.* **2009**, *131*, 6890.

(23) Koshima, H.; Takechi, K.; Uchimoto, H.; Shiro, M.; Hashizume, D. *Chem. Commun.* **2011**, *47*, 11423.
(24) Koshima, H.; Nakaya, H.; Uchimoto, H.; Ojima, N. *Chem. Lett.* **2012**, *41*, 107.
(25) Kobatake, S.; Takami, S.; Muto, H.; Ishikawa, T.; Irie, M. *Nature* **2006**, *446*, 778.
(26) Terao, F.; Morimoto, M.; Irie, M. *Angew. Chem., Int. Ed.* **2012**, *51*, 901.
(27) Morimoto, M.; Irie, M. *J. Am. Chem. Soc.* **2010**, *132*, 14172.
(28) Uchida, K.; Sukata, S.-I.; Matsuzawa, Y.; Akazawa, M.; de Jong, J. J. D.; Katsonis, N.; Kojima, N. Y.; Nakamura, S.; Areephong, J.; Meetsma, A.; Feringa, B. L. *Chem. Commun.* **2008**, 326.
(29) Al-Kaysi, R. O.; Müller, A. M.; Bardeen, C. J. *J. Am. Chem. Soc.* **2006**, *128*, 15938.
(30) Al-Kaysi, R. O.; Bardeen, C. J. *Adv. Mater.* **2007**, *19*, 1276.
(31) Bushuyev, O. S.; Singleton, T. A.; Barrett, C. J. *Adv. Mater.* **2013**, *25*, 1796.
(32) Finkelmann, H.; Nishikawa, E.; Pereira, G. G.; Warner, M. *Phys. Rev. Lett.* **2001**, *87*, 015501.
(33) Hogan, P. M.; Tajbakhsh, A. R.; Terentjev, E. M. *Phys. Rev.* **2002**, *E65*, 041720.
(34) Warner, M.; Mahadevan, L. *Phys. Rev. Lett.* **2004**, *92*, 134302.
(35) Corbett, D.; Warner, M. *Phys. Rev. Lett.* **2006**, *96*, 237802.
(36) Cviklinski, J.; Tajbakhsh, A. R.; Terentjev, E. M. *Eur. Phys. J.* **2002**, *E9*, 427.
(37) Dunn, M. L. *J. Appl. Phys.* **2007**, *102*, 013506.
(38) Kim, T.; Zhu, L.; Mueller, L. J.; Bardeen, C. J. *CrystEngComm* **2012**, *14*, 7792.
(39) A structure of **DR1**·H_2O was previously determined: Lacroix, P. G.; Malfant, I.; Iftime, G.; Razus, A. C.; Nakatani, K.; Delaire, J. A. *Chem.—Eur. J.* **2000**, *6*, 2599.
(40) From Figure 3, the radius is sum of the depth (h_{cr}) and the apothem (k_{cr}), $R = k_{cr} + h_{cr}$. Since $k_{cr}^2 + r^2/4 = R^2$, the apothem is $k_{cr} = (r^2 - 4h_{cr}^2)/8h_{cr}$. By substituting this value in $R = k_{cr} + h_{cr}$, for the radius and the curvature we obtain $R = (r^2 + 4h_{cr}^2)/8h_{cr}$ and $\kappa = 8h_{cr}/(r^2 + 4h_{cr}^2)$.
(41) The samples were irradiated with a medium-pressure UV lamp (SP-7, Ushio) equipped with a heat-cut filter that removes all wavelengths > 400 nm, and a standard reflector, for which the reflected intensity < 290 nm is negligible. Thus, the processes observed here are not due to heating effects or to secondary reactions which could be induced by high-energy UV radiation. The crystal motion was manually tracked by using the Hot Shot Link software (NAC Image Technology). To measure the size of the crystals, the software was properly calibrated by using a micrometer scale at the crystal position.
(42) Crystal #9 was selected as a convenient probe to verify the kinematic model because it responds to light with simple kinetics. Other crystals underwent dampened oscillations over time, which in addition to the photochemical kinetics that are treated here would require inclusion of differential equations that explicitly account for the anharmonicity of the restoring elastic force in slender beams that perform dampened oscillations. Analytical treatment of such involved model carries significant burdens and is out of the scope of this study where we focus on the effect of excitation on the kinematics of simple, monotonous bending and unbending.
(43) The bending moment corresponds to the average internal stress exerted on a structure element when the element bends under the action of an external force.
(44) Han, S. M.; Benaroya, H.; Wei, T. *J. Sound Vibr.* **1999**, *225*, 935.
(45) Boresi, A. P.; Schmidt, R. J.; Sidebottom, O. M. *Advanced Mechanics of Materials*; John Wiley and Sons: New York, 1993.
(46) Thomson, W. T.; Dahleh, M. D.; Padmanabhan, C.; Vlissides, J. *Theory of Vibration with Applications*, 5th ed.; Pearson: Upper Saddle River, NJ, 2008.
(47) Timoshenko, S. *J. Opt. Soc. Am. Rev. Sci. Instrum.* **1925**, *11*, 233.
(48) Timoshenko, S. *Theory of Elastic Stability*: McGraw Hill Book Co.: New York, 1956.
(49) Rosinger, H. E.; Ritchie, I. G. *J. Phys. D: Appl. Phys.* **1977**, *10*, 1461.
(50) Morimoto, M.; Irie, M. *Chem. Commun.* **2005**, 3895.
(51) Clyne, T. W.; Gill, S. G. *J. Therm. Spray Technol.* **1996**, *5*, 401.
(52) Abawi, A. T. *The Bending of Bonded Layers Due to Thermal Stress*; HRL: Malibu, CA, 2004.